Ionic Liquids-Cobalt (II) Thermochromic Complexes: How the Structure Tunability Affects "Self-contained" Systems

Floriana Billeci,[a,b] H. Q. Nimal Gunaratne,[b,c] Peter Licence,[d] Kenneth R. Seddon,[b,e] Natalia V. Plechkova,[b,f] Francesca D'Anna[*,a]

[a] Università degli Studi di Palermo, Dipartimento STEBICEF, Viale delle Scienze, Ed. 17, 90128 Palermo, Italy; email: francesca.danna@unipa.it; floriana.billeci@unipa.it.

[b] The QUILL Research Centre, School of Chemistry and Chemical Engineering, and [c] School of Chemistry and Chemical Engineering, Queen's University of Belfast, Stranmillis Road, Belfast, Northern Ireland BT9 5AG, UK; email: N.gunaratne@qub.ac.uk; n.plechkova@qub.ac.uk.

[d] GSK Carbon Neutral Laboratories, School of Chemistry, The University of Nottingham, Nottingham, UK; email: peter.licence@nottingham.ac.uk .

[e] Deceased

[f] Welcome-Wolfson Institute for Experimental Medicine, School of Medicine, Dentistry and Biomedical Sciences, The Queen's University Belfast, 97 Lisburn Road, BT9 7BL Belfast, U.K.

Corresponding Author

*Email: francesca.danna@unipa.it

Abstract

With the aim of obtaining thermochromic systems with potential applications in solar energy storage, we evaluated the behaviour of some sugar based ionic liquids-$Co(NTf_2)_2$ complexes, in ionic liquids solution, as a function of temperature. Different structural changes on the cation, the nature of the anion, as well as the nature of the ionic liquid used as solvent were considered.

The analysis of the above factors was carried out through a combined approach of different techniques, *i.e.* variable temperature (VT) UV-vis and NMR spectroscopies, conductivity and thermal gravimetric analysis. The thermochromic systems were analysed both as solutions and

as thin films and the data collected highlights the defining role played by both the cation structure and the solvent nature in determining their performance.

Most of the investigated systems show a chromogenic transition from pink to blue, occurring in a temperature range suitable for practical applications (40-60 °C). Interestingly, when embedded in a polymeric matrix, thin films with high recyclability and long life are also described.

Introduction

The ever-increasing global energy demands, due to expanding developments and increasing populations, have led to serious scrutiny over the depleting energy resources. Global energy demand has focused attention on a sustainable energy generation coupled with optimized use of energy, minimized pollution and limiting fossil fuel-based energy consumption to a bare minimum. These aspects have led to an increasing focus on the short-term stored energy resources, which could be derived from wind power, hydropower, solar power, biomass, *etc*. Solar energy is a viable and inexhaustible source of energy[1] for generating power, with the aid of solar cells, and harnessing its heat *via* efficient storage of sun's heat using compounds/materials with high heat capacities. In relation to this, it is a major challenge to store energy due to daily and seasonal variations in the accessibility of sunlight. The schemes generally known as molecular solar thermal (MOST) systems, for example phase changing materials that store energy in the form of lattice energy, represent a promising avenue for harvesting and storing solar energy.[2-4] In this context, photochromic systems where a molecule is converted by photoisomerization into a higher-energy isomer, which is capable of storing the energy until released by a trigger, converting the meta-stable isomer to the original light-harvesting isomer,[5-9] have played a significant role.

Thermochromism, defined as reversible change in the color of a compound when it is heated or cooled, has received little attention as an energy harvesting mechanism.[10-12] The thermochromic color change of a compound/material is distinguished often by eye, and occurring over a small or sharp temperature interval. For inorganic compounds this transition is frequently due to a change in crystalline phase, to a change in ligand geometry, as a result of a charge transfer,[13] modifications in the chemical structure,[14] or to a change in number of molecules of solvent in the first coordination sphere.[15,16] A fewer known examples are as a result of equilibria between complexes in solution or to equilibria between different molecular

structures in the case of organometallic compounds.[17] The thermochromic transition temperature of a pure substance may be greatly changed by dispersing the compound in a solid matrix or by mixing it with other substances. Widely used matrices include waxes, and polymers which are compatible with the thermochromic substance. In the solid matrix, a hysteresis effect of color transition may be affected by the nature of the matrix. In this context, thermochromic substances, embedded in coatings, are beginning to surface in the design of new materials for energy saving.[18-20] In some cases, the percentage of energy savings reached to more than 16%.[21] Looking specifically at thermochromic transition metal complexes, the states with different coordination numbers are shown to be in equilibrium with the ligand or solvent molecules where the increase in temperature generally favours the lower-coordinated complex.[22]

Among transition metal complexes, thermochromism of cobalt is the most widely known and has been studied in different solvent systems.[15,23] Gadzuric *et al.* examined the thermochromic phenomena of cobalt(II) chloride complexes in $NH_4NO_3 \cdot zNMF$ (N-methylformamide) ($z = 3, 4, 5, 6$ and 20) solution, in the temperature range of 33–73 °C, who showed the insertion of chloride ion in the metal coordination sphere, favours the transition from an octahedral to a tetrahedral geometry inducing a colour change.[24] However, these kind of systems, involving a ligating volatile solvent, are often not self-contained as the phenomenon depends on the addition or removal of (solvent) ligands where water is a commonly used solvent.[25] The key challenging issues regarding such thermochromic systems involving metal complexes are the volatility of the solvent used while maintaining a viable temperature range where the transformation occurs.

In this context, ionic liquids (ILs) present a viable alternative to ligating solvents with their high thermal stability and desirable structure tunability,[24,26] allowing their application in different fields.[27-29] Moreover, the associated anions in ILs can be chosen to adjust coordination capability towards metal ions. In this regard, imidazolium based ILs have been used in combination with Ni(II) salts, both in solutions and thin films, to obtain systems that show a thermochromic transition from green to blue, in the temperature range 35-65 °C or room temperature-120 °C.[30-32] Furthermore, imidazolium ILs have also been used in combination with Co(II) salts, giving systems in which the thermochromic switch occurs under room[33 34 35] or sub-zero temperatures or alternatively at very high temperatures.[35-37] These transition temperatures limit the use such IL-Metal complexes within the solar thermal energy range. To overcome such limitations, we have recently introduced a self-contained IL-Co(II) system[38] where the ILs were synthesised from a sugar-based source (derived from food waste), utilising

a simple reaction scheme. It was found to be compatible with some polymer matrixes allowing the fabrication of composite systems for real-life applications. We hypothesised that solar thermal energy can be absorbed and stored in the high energy state of the thermochromic system and subsequently emitting the stored heat during the return to a low energy state.

Here, we report a detailed investigation of the system examining the thermochromic interactions occurring between sugar-based ILs, acting as ligands, and a cobalt salt, $Co(NTf_2)_2$ (Scheme 1), in particular, IL ligands bear gluconic functionality in the cation structure. The IL ligands, when taken into consideration differ in the alkyl chain length, varying from butyl to dodecyl chains. In the case of the octyl derivative, the effect of alkyl chain branching was also considered, using both linear octyl and a 2-ethylhexyl derivative. Furthermore, cations also differ in the length of the spacer between the amide and ammonium functionalities. As for the anion effect, both bromide and iodide salts were used. The synthesis and toxicological aspects of these IL ligands have been recently investigated, demonstrating that this class of ILs show both low cyto- and ecotoxicities.[39]
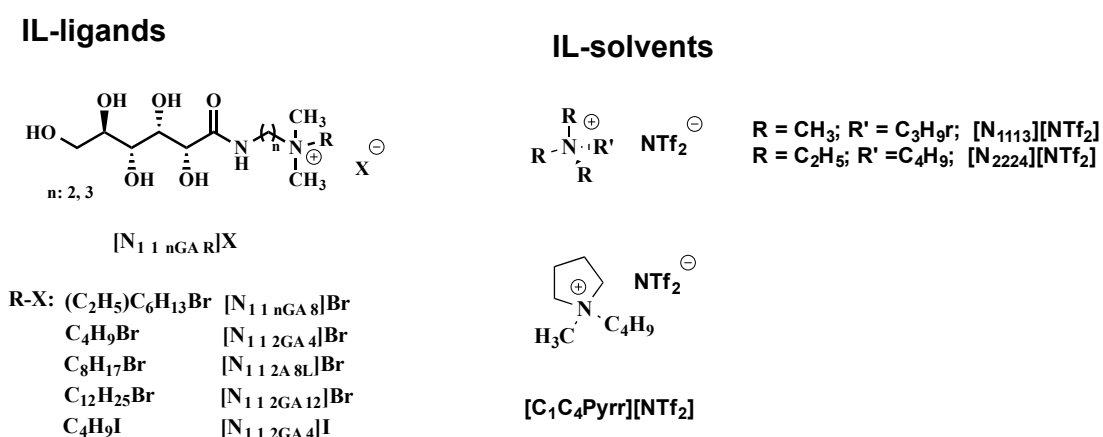
**Scheme 1.** Structures of the ILs investigated in this work.

IL-based thermochromic systems obtained show transitions in the useful temperature range of 40-60 °C and demonstrate the significant effect that structural changes on the ions exert on their performance. The systems were analysed both in solution and in polymeric films, opening the way to elucidating the parameters driving the thermochromic systems to suit any prospective applications.

Results and Discussion

UV-vis investigations. As stated above, the system $[N_{1\,1\,2GA\,8}]Br/Co(NTf_2)_2$ (3:1) was previously investigated in $[N_{2\,2\,2\,4}][NTf_2]$ solution (from now on, systems will be indicated as IL-ligand/$Co(NTf_2)_2$/IL solvent n:1, where n indicates the molar ratio ligand/$Co(NTf_2)_2$).[38] The need for using a solvent came from the high viscosity of the IL ligand which made a direct investigation of the complex more difficult. The solution obtained showed a colour transition from pink to blue at 59 °C (T_{switch}) and this change was ascribed to a variation of the complex geometry from octahedral (O_h) to tetrahedral (T_d). The above hypothesis was also confirmed by the determination of the magnetic momentum (μ_{eff}). Furthermore, a previous investigation demonstrated the need to have the presence of the gluconic moiety in the ligand, to observe the thermochromic transition.

Bearing in mind the above result, we firstly investigated the effect of the ligand/metal molar ratio that can potentially affect the establishment of equilibrium. In particular, the above parameter was changed from 1.5 up to 7. Figures 1 and S1-S3 show the UV-vis spectra, trend of absorbance as a function of the temperature and colour shades for the corresponding solutions.

UV-Vis measurements were performed in the range 15-90 °C, with the exception of the highest molar ratios (6 and 7) for which a starting temperature of 30 °C was used as a consequence of the opalescence of the solutions observed at low temperature.
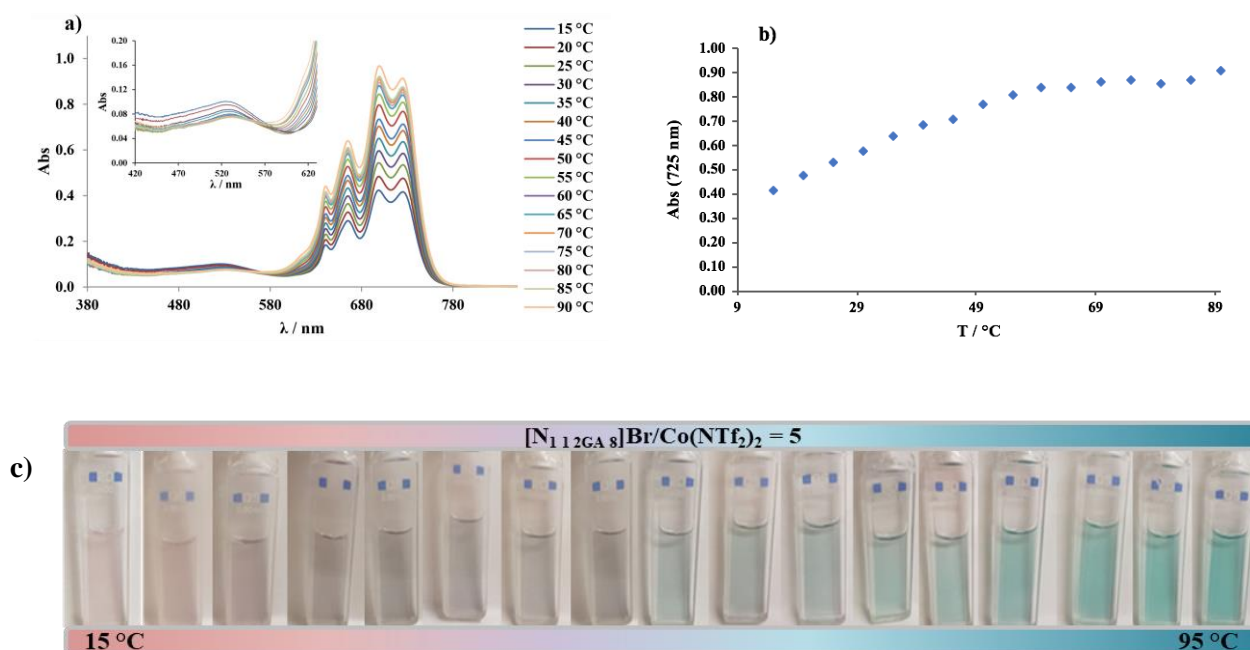
Figure 1. a) UV-vis spectra of [N$_{1\ 1\ 2\ GA\ 8}$]Br/Co(NTf$_2$)$_2$/[N$_{2224}$][NTf$_2$] at ligand/metal molar ratio equal to 5 (inset: high energy band); b) trend of absorbance at 725 nm as a function of temperature; c) colour shades.

It should be noted that at the lowest molar ratio (1.5), a thermoreversible system was not obtained. The suspension, firstly pink in colour, became a clear blue solution after heating, maintaining this colour also after cooling. This was confirmed by the absence of variations in the UV-vis spectra with the raise in temperature (Figure S1a).

In all the other cases, spectra show two set of different bands, the first one located in the range 450-600 nm and the second in the range 600-800 nm. According to previous reports, the band at the lower wavelength is related to the octahedral complex (O$_h$) whose weak absorption is in line with the Laporte rule.[40] The second high absorption band can be related to the tetrahedral complex (T$_d$) which, lacking a centre of symmetry, featured a strong absorption that can also be related to its concentration. Raising the temperature, a decrease in the intensity of the high-energy band and a corresponding increase in intensity of the low-energy band was observed, according to the occurrence of an equilibrium process. The above hypothesis was further supported by the detection of isosbestic points, whose position moved at longer wavelengths as a function of the molar ratio: 550 nm[38]- 561 nm - 605 nm - 633 nm for the molar ratio 3, 5, 6, 7 respectively. According to a previous report, this hypsochromic shift can be related to the amount of ligand available in the solution that, in turn, affects the amount of precursor that is converted into the product,[41] inducing a faster and easier formation of the tetrahedral complex.

Analysis of the absorbance values, at 725 nm, as a function of temperature gives the trends reported in Figures 1b and S2. These trends show changes in the slope and the temperatures (T_{switch}, Table 1), obtained by extrapolation, corresponding to the point of intersection of the two straight lines and representing visible changes in the colour of the solution due to the O_h-T_d switching.

Table 1. Temperature of the geometry switch for the system $[N_{1\,1\,2GA\,8}]Br/Co(NTf_2)_2/[N_{2\,2\,2\,4}][NTf_2]$ at different ligand/metal molar ratios and using different ILs as solvent

Entry	Thermochromic system	Ratio [ligand]/[metal]	T_{switch} °C[a]
1	$[N_{1\,1\,2GA\,8}]Br/Co(NTf_2)_2/[N_{2\,2\,2\,4}][NTf_2]$[38]	3:1	59
2	$[N_{1\,1\,2GA\,8}]Br/Co(NTf_2)_2/[N_{2\,2\,2\,4}][NTf_2]$	5:1	56
3	$[N_{1\,1\,2GA\,8}]Br/Co(NTf_2)_2/[N_{2\,2\,2\,4}][NTf_2]$	6:1	82
4	$[N_{1\,1\,2GA\,8}]Br/Co(NTf_2)_2/[N_{2\,2\,2\,4}][NTf_2]$	7:1	55 and 89
5	$[N_{1\,1\,2GA\,8}]Br/Co(NTf_2)_2/[C_1C_4pyrr][NTf_2]$	3:1	44
6	$[N_{1\,1\,2GA\,8}]Br/Co(NTf_2)_2/[N_{1\,1\,3}][NTf_2]$	3:1	57

[a]T_{switch} were reproducible within 1 °C.

The increase in the molar ratio affected T_{switch} values. Indeed, the above parameter stayed almost constant increasing the molar ratio from 3 up to 5 (entries 1-2), but with a further increase in the molar ratio, the above parameter moved T_{switch} to higher values, 82 °C (entry 3) for a ratio of 6 and 55 and 89 °C for the highest ratio (entry 4). Interestingly, in this case, at 55 °C, the solution with the molar ratio (7:1) appeared to be light blue in colour, but increasing the temperature, it became a deeper blue. Probably, the obtained result can be ascribed to the increase in the viscosity of solution, due to the presence of a larger amount of ligand, consequently slowing down the establishment of the equilibrium.

Among analysed systems, the $[N_{1\,1\,2GA\,8}]Br/Co(NTf_2)_2$ with molar ratio (3:1) showed the best performance and it was selected to optimize all the other experimental parameters.

In the attempt to improve system performance, we investigated the effect of solvent nature using $[N_{1\,1\,3}][NTf_2]$ and $[C_1C_4pyrr][NTf_2]$ (Scheme 1). With respect to the previously used

IL, $[N_{1113}][NTf_2]$ exhibited a lower viscosity (72.0 cP and 104 cP, at 25 °C, for $[N_{1113}][NTf_2]$[42] and $[N_{2224}][NTf_2]$[43] respectively). On the other hand, $[C_1C_4pyrr][NTf_2]$ had a comparable viscosity to $[N_{1113}][NTf_2]$ (72 cP, at 25 °C),[44] but with a different cation structure. Also, in this case, macroscopic colour changes were observed together with significant variations in the UV-vis spectra (Figures S4-S5). However, in contrast to that which was detected in $[N_{2224}][NTf_2]$ solution, in both cases, the band related to the octahedral geometry was less pronounced and the trend of absorbance as function of temperature showed a more gradual change in slope.

The analysis of the T_{switch} values (Table 1, entries 4-5) sheds light on the major role played by the IL cation structure, rather than the viscosity. Indeed, the transition temperature stayed unchanged when going from $[N_{2224}][NTf_2]$ to $[N_{1113}][NTf_2]$ notwithstanding a decrease in the solvent viscosity. Conversely, it significantly decreased down to 44 °C, changing the solvent from $[N_{1113}][NTf_2]$ to $[C_1C_4pyrr][NTf_2]$, despite the lower differences in viscosity. Probably, a cation with a more organised structure and a lower conformational flexibility, like $[C_1C_4pyrr]^+$, interferes less with the occurrence of changes in the metal coordination sphere that are necessary to favour the transition from the octahedral to the tetrahedral complex. This gives rise to a system more suitable for a practical application, considering that the change in colour occurs at a temperature that can be reached during hotter days in the summer.

The last factor we considered was the effect deriving from structural changes on the ligand (cation). On this subject, it is noteworthy that the structural variation may pertain to the length of the spacer between the ammonium and the amide functionalities or the nature (length and branching) of the alkyl chain on the ammonium cation and the anion.

Firstly, we analysed the effect due to the spacer, using the $[N_{113GA8}]Br$ (Figures S6a-b). Also in this case, a reversible colour change was observed with an isosbestic point at 576 nm that was bathochromically shifted by 30 nm with respect to the one detected in the presence of $[N_{112GA8}]Br$.[38]

Interestingly, the change in slope occurred at 45 °C, reflecting a colour switch from pink to light blue, but a net gap in the absorbance value was also detected at 79 °C, corresponding to the complete transition to tetrahedral geometry and a blue colouration of the solution. The observed transition accounts for the positive role played by the elongation of the spacer, leading to the increased conformational flexibility, which allows an easier rearrangement of the ligand in the metal coordination sphere.

Further investigation aimed at assessing the effect exerted by the nature of the alkyl chain on the ammonium head, using ligands like [N$_{1\ 1\ 2\ GA\ 8L}$]Br, [N$_{1\ 1\ 2GA\ 4}$]Br and [N$_{1\ 1\ 2GA\ 12}$]Br, gave no pronounced thermochromic effects (Figure S6c-f). Indeed, in all cases, the above structural changes suppressed the thermochromic behaviour; a blue solution, representative of the predominance of the tetrahedral complex, was obtained at room temperature and maintained its colouration also after cooling.

Finally, to investigate the role played by the nature of the anion ligand, we bore in mind results previously collected demonstrating that changing the bromide ion with a non-coordinating ion, like [NTf$_2$]$^-$, suppressed the thermochromic behaviour.[38] Consequently, we used an anion having an intermediate coordination ability, like iodide ion, and using the [N$_{1\ 1\ 2GA\ 4}$]$^+$ cation, we obtained a yellow solution which was obtained at room temperature, that gradually turned to green upon increasing the temperature.(Figure 2).
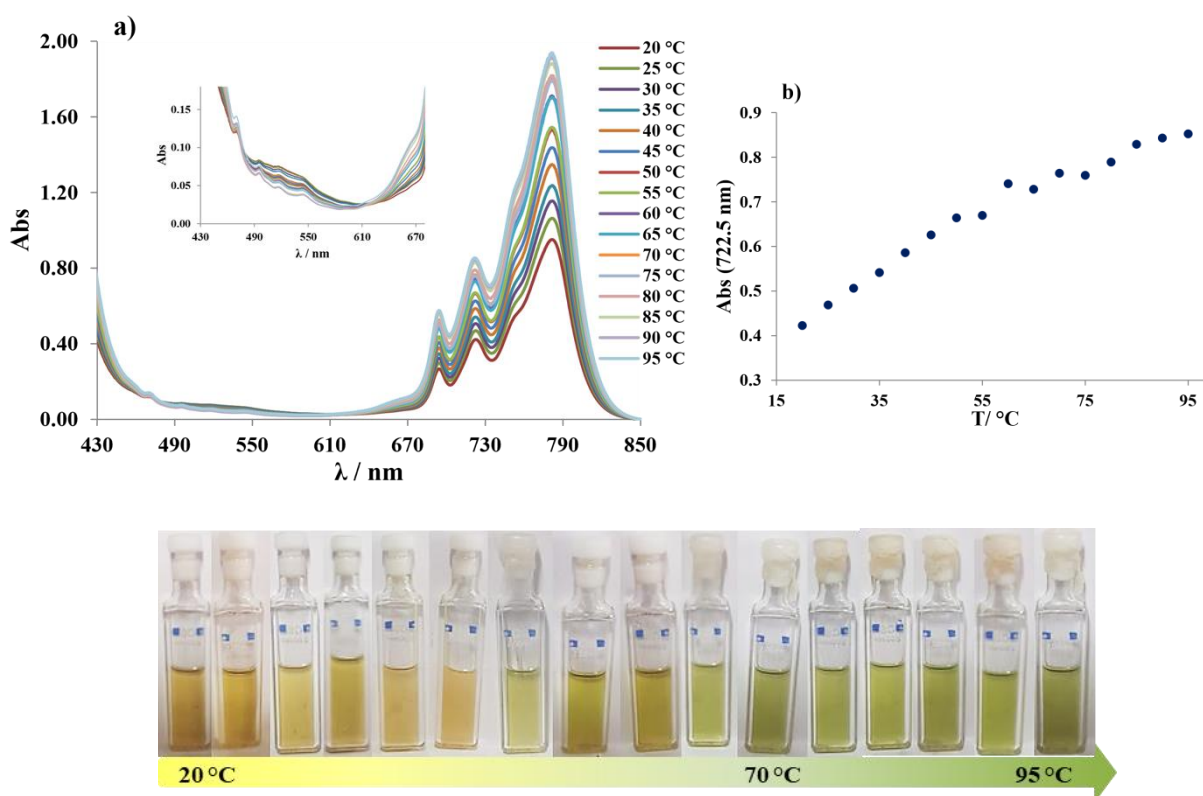

Figure 2. a) UV-vis spectra (inset: high energy band); b) trend of absorbance as a function of the temperature; c) color shades for the system [N$_{1\ 1\ 2GA\ 4}$]I/Co(NTf$_2$)/[N$_{2\ 2\ 2\ 4}$][NTf$_2$] (3:1).

Analysis of the spectra recorded as a function of the temperature shows some interesting features. Firstly, in the region of the tetrahedral complexes, the bands were bathochromically shifted and the one occurring in the range 750-850 nm was quite enlarged. Superimposed

spectra allowed the detection of the occurrence of two isosbestic points at 479 and 615 nm. Furthermore, the colour change was gradual (Figure 2c) and in the trend of absorbance as a function of temperature (Figure 2b), a change in slope was detected at 55 °C. The above results seem to be indicative of a different interaction between the metal centre and the ligand, with respect to the one indicated in the case of $[N_{1\ 1\ 2GA\ 8}]Br$. Probably, the yellow colour indicated the first interaction between the 'soft' iodide ion and Co(II), further supported by the cooperation of the amide functionalities present on the cation structure. According to previous reports in literature, [45] [46] the colour transition from yellow to green could be ascribed to the reorganisation in the Cobalt coordination sphere, in which the cation participation becomes predominant through a more significant involvement of amide groups. In order to verify that change in colour was not due to the formation of I_3^-, a sample of the thermochromic system was added with an equimolar amount of NaSCN. After heating and cooling, the resulting sample retained its thermochromic behaviour effectively eliminating the suggested presence of an iodide complex.

UV-vis investigation was also used to obtain insight on the complex stoichiometry. To this aim, Job's plots were obtained for $[N_{1\ 1\ 2GA\ 8}]Br/Co(NTf_2)_2/[N_{2\ 2\ 2\ 4}][NTf_2]$ and $[N_{1\ 1\ 3GA\ 8}]Br/Co(NTf_2)_2/[N_{2\ 2\ 2\ 4}][NTf_2]$, on the grounds of their relatively low transition temperatures.

Measurements were performed both at 25 and 70 °C and the trend of absorbance as a function of the Co(II) mole fraction (X_{Co}) are reported in Figures 3 and S7.
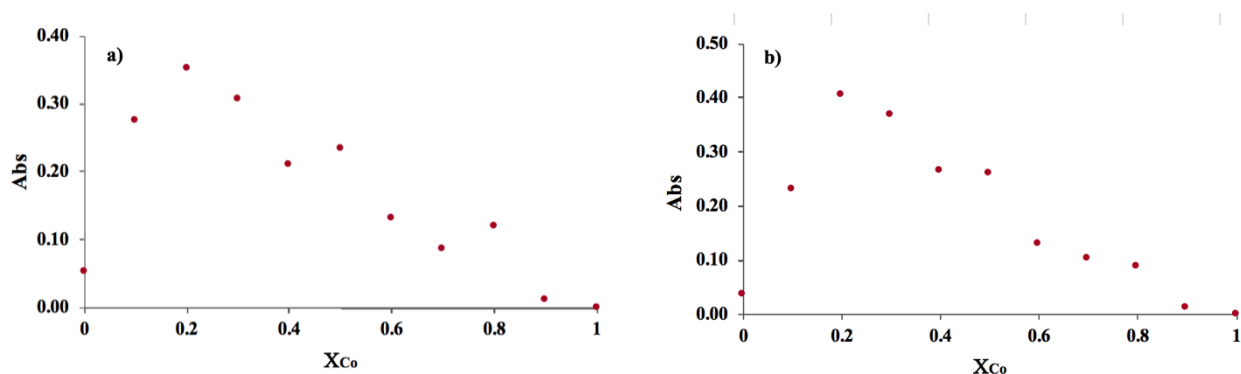
Figure 3. Job plots (ΔA vs. X_{Co}) for the system $[N_{1\ 1\ 3GA\ 8}]Br/Co(NTf_2)_2/[N_{2\ 2\ 2\ 4}][NTf_2]$ at a) 25 °C (λ: 712 nm); b) 70 °C (λ: 713 nm).

Analysis of the above plot reveals some interesting features. Firstly, the two ligands exhibit different binding abilities as accounted for by the different shape of the obtained plots. In particular, according to previous reports,[47] in the case of $[N_{1\ 1\ 3GA\ 8}]Br$ a sharp plot was obtained

(Figure 3), while for $[N_{1\ 1\ 2GA\ 8}]Br$ a bell-shaped curve was recorded (Figure S7), accounting for a strong binding ability in the first case, more so than in the second case.

In the case of $[N_{1\ 1\ 3GA\ 8}]Br/Co(NTf_2)_2$, the position of the maximum was at $\sim X_{Co} = 0.25$ indicating a metal/ligand 1:3 stoichiometric ratio. Contrarily, for $[N_{1\ 1\ 2GA\ 8}]Br/Co(NTf_2)_2$, the maximum of the Job's plot occurred at $\sim X_{Co} = 0.3$, accounting for a 1:2 stoichiometric ratio.

The maximum position did not change by rising the temperature, indicating that the thermochromic behaviour is not related to a change in the number of the ligand molecules involved in the complex, but rather to the number and nature of chemical functionalities borne on the ligand participating in the interaction.

Magnetic susceptibility investigations. The systems obtained were also characterised from a magnetic point of view, determining the magnetic susceptibility. In the case of transition metal complexes, this kind of investigation provides information about the complex geometry, as the distribution of unpaired electrons in the d-orbitals determines the properties of the complex formed.[48]

To this aim, the Evans method is an indirect method to calculate the magnetic moments (μ_{eff}) through magnetic susceptibility,[49] on the grounds of the magnetic response of a probe compound in the presence and absence of the sample. (see Supporting Information for details).

This kind of investigation was previously performed on the $[N_{1\ 1\ 2GA\ 8}]Br/Co(NTf_2)_2/[N_{2\ 2\ 4}][NTf_2]$ (3:1) system and confirmed the interconversion between the octahedral and tetrahedral complexes induced by the increase in temperature.[38]

With the above information in mind, we firstly investigated the $[N_{1\ 1\ 3GA\ 8}]Br/Co(NTf_2)_2/[N_{2\ 2\ 4}][NTf_2]$ (3:1) system, using t-butanol as the probe, as reported earlier.[38] Unfortunately, after the t-butanol addition, the solution became immediately blue and the calculated μ_{eff} values at different temperatures (Table S1) stayed almost constant (Figure S8a-b).

Different results were collected using DMF as the probe compound. Indeed, in this case, the raise in temperature produced a significant difference in the chemical shift ($\Delta\delta$) and produced a variation in the μ_{eff} values (Figure 4).
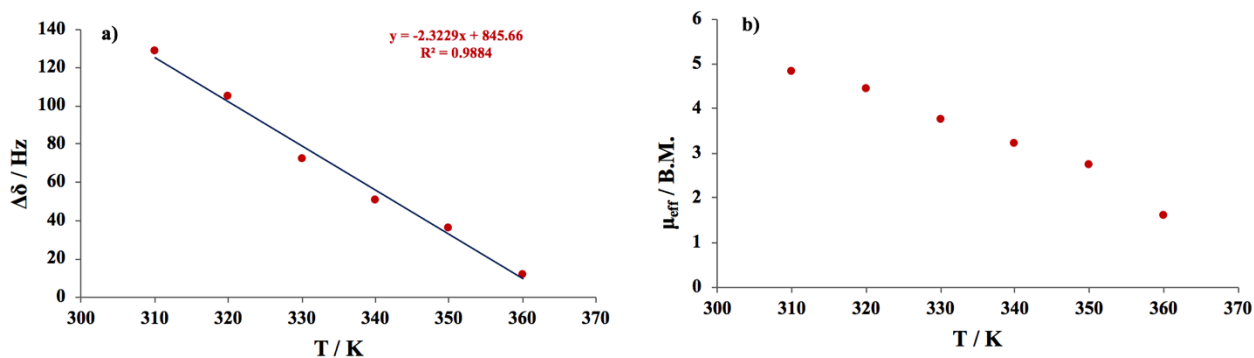
Figure 4. Trends of: a) $\Delta\delta$ as a function of temperature; b) μ_{eff} as a function of the temperature for [N$_{1\ 1\ 3GA\ 8}$]Br/Co(NTf$_2$)$_2$/[N$_{2\ 2\ 4}$][NTf$_2$] (3:1)– DMF system.

The magnetic moment gradually decreased, raising the temperature and affecting the values collected up to 40 °C, perfectly accounting for an octahedral geometry (Table S1). However, further increases in temperature induced a significant decrease in μ_{eff}, becoming similar to those obtained using *t*-butanol as a probe compound, this according to previous reports,[50][51] is indicative of a tetragonal distortion of the original geometry.

The investigation was also performed in the presence of [N$_{1\ 1\ 3GA\ 4}$]I and the data collected confirmed that the yellow to green colour transition corresponded to an octahedral-tetrahedral geometry interconversion (Figure S8c-d). The values obtained (Table S2) match with the high spin complexes with an electronic distribution for the octahedral geometry $t_{2g}^5 e_g^2$ that corresponds to the ground term ^{4}T. Increasing the temperature, the tetrahedral geometry reorganisation determines the electronic configuration $e^4 t_2^3$, for a ground term ^{4}A.[52] Interestingly, the μ_{eff} corresponding to a tetrahedral geometry was obtained at 70 °C, in perfect agreement with the macroscopic colour change and UV-vis investigation.

NMR investigations. The thermochromic systems were further analysed taking advantage of the magnetic active nature of cobalt. Indeed, ^{59}Co NMR has been widely used to investigate a wide range of different complexes, irrespective of the quadrupolar spin number of cobalt (S = 7/2) that frequently gives a broad peak, which is difficult to observe.[53,54]

In general, changes in the structure of cobalt complexes due to internal or external factors, above all if induced by the temperature, affects the chemical shift values. On this subject, Ozvat *et al*., took advantage of the correlation between of the ^{59}Co chemical shift and temperature to perform thermometry via magnetic resonance imaging.[55] They investigated $\Delta\delta/\Delta T$ for nuclei of low-spin Co(III) complexes, correlating the degree of ligand encapsulation within the 1st coordination sphere with the amplification of temperature sensitivity.

The VT ^{59}Co NMR investigation was performed in the temperature range 30 – 90 °C, in line with the VT UV-Vis measurements. Chemical shift values (δ) were collected using the diamagnetic external standard $K_3[Co(CN)_6]$ having a formal charge on Cobalt equal to 3+. The external standard exhibits changes in chemical shift as a function of the temperature with a coefficient of 6.2 Hz °C^{-1}.[56] However, changes in chemical shift for the systems investigated were three orders of magnitude larger than the ones for the reference signal, avoiding the need to consider corrections to the chemical shift values for the samples.

Data previously collected for $[N_{1\ 1\ 2GA\ 8}]Br/Co(NTf_2)_2/[N_{2\ 2\ 2\ 4}][NTf_2]$ (3:1) shed light on the perfect correspondence between T_{switch} detected by UV-vis investigation and the change in slope occurring in the trend of $\varDelta\delta$ as a function of the temperature, supporting the hypothesis that macroscopic colour changes can be ascribed to change in the structure of the complex.[38] Now the effect of the amount of ligand was taken in consideration, using a ligand/metal molar ratio equal to 7 (Figure 5).
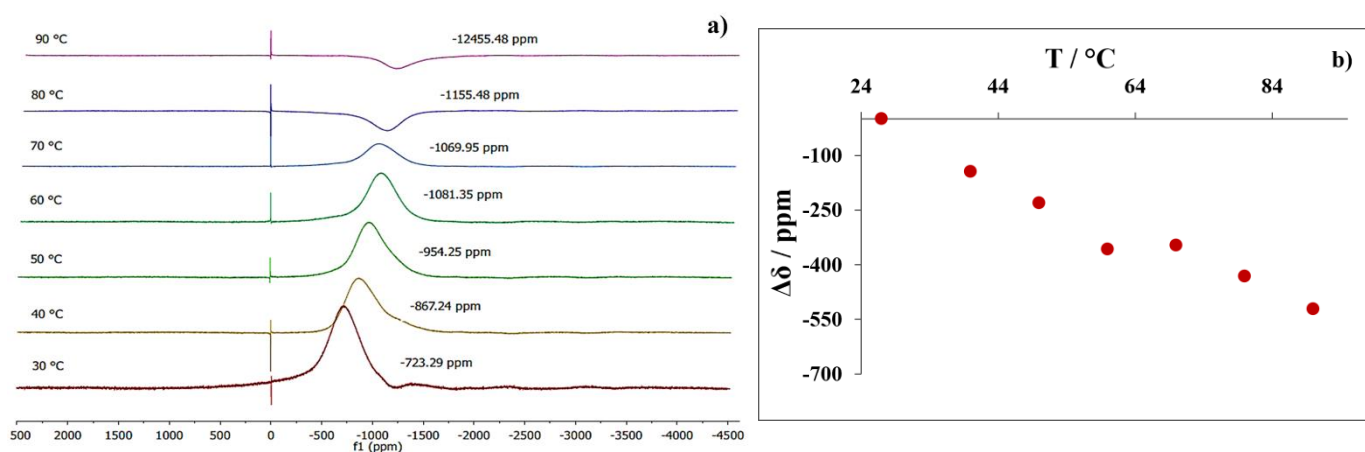
Figure 5. VT ^{59}Co NMR for the system $[N_{1\ 1\ 2GA\ 8}]Br/Co(NTf_2)_2/[N_{2\ 2\ 2\ 4}][NTf_2]$ (7:1) **a)** spectra recorded in the range 30 – 90 °C (^{59}Co signal for $K_3[Co(CN)_6]$ fixed at 0 ppm); **b)** trend of $\varDelta\delta$ as a function of the temperature in the range 30 – 90 °C.

Analysis of NMR spectra accounts for the significant change in chemical shift with the temperature increase. Interestingly, raising the temperature, an upfield shift was detected with an inversion of phase of the signal in the range 70-80 °C. On the other hand, the trend of $\varDelta\delta$ as a function of temperature exhibited a plateau region in the range 60-70 °C, in perfect agreement with data collected by UV-vis investigation.

To have insight on the effect exerted by the different structural features, the investigation was carried out on $[N_{1\ 1\ 3GA\ 8}]Br/Co(NTf_2)_2$, and $[N_{1\ 1\ 2GA\ 4}]I/Co(NTf_2)_2$ (3:1) (Figure S9). In all

cases, an upfield shift of the ^{59}Co signal with the temperature increase was detected. $\Delta\delta$ values show changes in slope in temperature ranges perfectly matching the ones detected in the UV-vis investigation, confirming that the occurrence of the colour change was due to variations in the metal coordination sphere.

Thermochromic films. The main aim of this work was to verify if the systems obtained could be deployed as components for energy-storage devices. This goal can be achieved by using thin films and currently this aim is an open research topic. On this regard, Yu *et al.* developed a nanocomposite hydrogel thermochromic film using pyridinium-modified polyacrylamide networks integrating with EGP5 (ethylene glycol-modified pillar[5]arene) and ATO nanoparticles (antimony-tin oxide). The system was featured by a transition temperature of 32.1 °C and the presence of a polymeric component to avoid the collapse of the hydrogel structure conferring to the system repeatability and durability.[57] In the same way, Salamati *et al.* used a sol-gel method to dope with W^{6+} ions and TiO_2 a PVP-VO_2 film, which was both thermochromic and photochromic.[58]

Among the factors affecting the performance of thin films, the concentration of the components plays a pivotal role. In this regard, Liu *et al.* incorporate carbon nanotubes (CNT) in polyethylene terephthalate (PET) obtaining a film whose response time to thermal solicitation was dependent on the quantities of CNT and PET.[59]

With the above information in mind, we considered the system $[N_{1\,1\,2GA\,8}]Br/Co(NTf_2)_2$ (3:1) and prepared thin films gradually decreasing the amount of PMMA (from 340 down to 290 mg; the mass fraction of polymer in the thin film ranged from 85 down to 81%). In all cases, we obtained homogeneous films showing different thermochromic performance. Indeed, registration of the UV-vis spectra as a function of temperature, evidences a gradual increase in the spectra baseline at lower wavelengths. However, the bands corresponding to the tetrahedral complex (600-800 nm) were well defined (Figures S10-S11) and the trends of absorbance as a function of temperature showed a change in slope at about 40 and 55 °C for films prepared in the presence of 83 and 81% of PMMA. In contrast to data previously reported,[38] where the PMMA had a negligible effect on the thermochromic transition, here, the polymer significantly influenced features, as the films became less transparent (Figure S10-11).

The same investigation was also performed on the system $[N_{1\,1\,3GA\,8}]Br/Co(NTf_2)_2$ (3:1), with polymer mass fraction ranging from 84 down to 81%. UV-vis spectra and the trend of absorbance as a function of the temperature are reported in Figure 6.
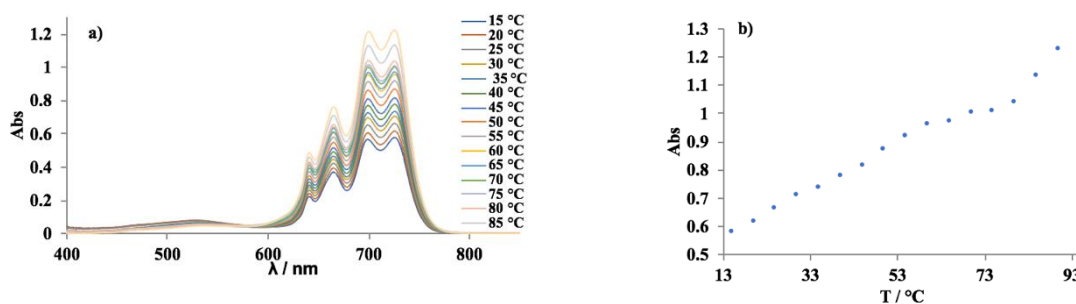
Figure 6. VT UV-Vis measurement for the polymeric film [N$_{1\,1\,3GA\,8}$]Br/Co(NTf$_2$)$_2$/PMMA (3:1) (390 mg; 84% of PMMA): a) spectra in the range of temperature 20-90 °C; b) trend of the absorbance increasing the temperature.

The absorbance of the polymeric film was much lower than the one detected in solution (Figure 6). However, the trend of absorbance as a function of the temperature perfectly agrees with the ones obtained in solution, showing a change in slope occurring at about 50 °C (Figure 6b) and confirming that also in this case thermochromic performance was retained in the polymer film. Furthermore, the film was transparent both at 25 and 80 °C, but different in colour (Figure 7).

Figure 7. Thermochromic polymeric film [N$_{1\,1\,3GA\,8}$]Br/Co(NTf$_2$)$_2$/PMMA (3:1) (390 mg): a) 25 °C; b) 80 °C.

The amount of PMMA was changed using both 83 and 81% of polymers (Figures S12-13). The decrease in the polymer amount led to non-homogeneous and less transparent films, without affecting the thermochromic transition that always occurred in the 55-60 °C range. However, as transparency is a qualification for this kind of systems, the better performing systems were clearly the ones containing the highest amount of polymer (85 and 84% of PMMA for [N$_{1\,1\,2\,GA8}$]Br/Co(NTf$_2$)$_2$ and [N$_{1\,1\,3\,GA8}$]Br/Co(NTf$_2$)$_2$, respectively).

Bearing in mind this information, we assessed the reusability of the film obtained using the thermochromic complex $[N_{1\,1\,3\,GA8}]Br/Co(NTf_2)_2$ (3:1). Indeed, possible recycling and long-term life are essential features for such kind of thermochromic coatings. Thin film was heated to 60 °C and UV-vis spectra were recorded. Interestingly, we were able to reuse the film for 42 cycles over three months, without any loss in performance (Figure 8).
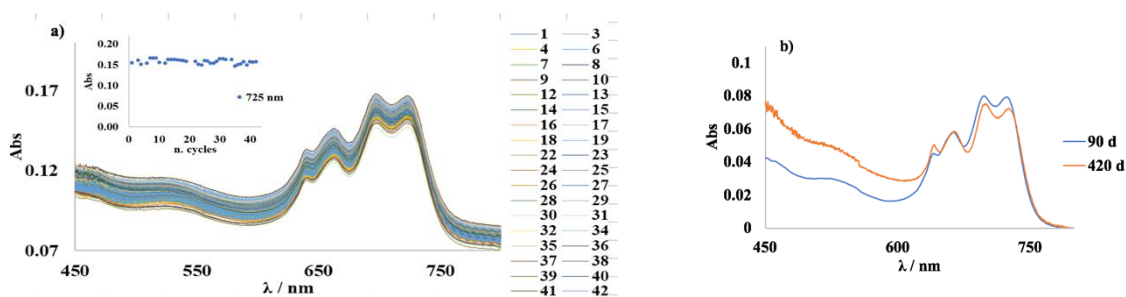
Figure 8. UV-vis spectra recorder for $[N_{1\,1\,3GA\,8}]Br/Co(NTf_2)_2$ (3:1)/PMMA film at 60 °C (inset: absorbance at 725 nm as a function of number of cycles); b) UV-vis spectra after 90 and 420 days.

To our surprise, after storage in air for 420 days after the last cycle, UV-vis spectrum did not show significant variations, further supporting the suitability of such system in a real application.

The above films were consequently investigated for their thermal stability, as thermal degradation can occur as a consequence of the stress of the material due to the consecutive heating-cooling cycles. Thermograms for neat polymer and thin polymeric films are displayed in Figure S14, while temperatures corresponding to a 5% of weight loss (T_d) are reported in Table 2.

Table 2. Temperature of degradation (T_d) corresponding to the 5% of weight loss for the PMMA and the films casted.

Film	T_d (°C)
PMMA	290 °C
$[N_{1\,1\,2GA\,8}]Br/Co(NTf_2)_2$/PMMA	238 °C
$[N_{1\,1\,3GA\,8}]Br/Co(NTf_2)_2$/PMMA	276 °C

In general, the incorporation of the thermochromic systems in the polymeric matrix induces a decrease in the thermal stability with respect to PMMA. Our thermochromic films were stable

at temperatures higher than 200 °C, warranting their practical applications, also considering that their colour transition occurs at much lower temperatures. Interestingly, the data collected indicates that the thermal stability is affected by the nature of the thermochromic system, with the ones incorporating $[N_{1\,1\,3GA\,8}]Br/Co(NTf_2)_2$ (3:1) in PMMA exhibiting the highest thermal stability.

Conductivity measurements. To have insight on the effect of the ligand structure on the conductivity of the systems, an investigation was performed on both the thermochromic solutions and the films. In particular, the two ligands showing the most interesting behaviour were considered, namely $[N_{1\,1\,2GA\,8}]Br$ and $[N_{1\,1\,3GA\,8}]Br$. The conductivity (σ) was determined through potentiostatic measurements, and these were carried out as a function of the temperature, covering the range 25-70 °C, to obtain information about the contribution deriving from the presence of the octahedral or tetrahedral complex. In all cases, besides the thermochromic system, contributions deriving from using IL as a solvent and ligand in IL solution were considered and, in the case of the complex system a (3:1) ligand/metal stoichiometric ratio was used. Data collected as a function of temperature are shown in Figure 9.
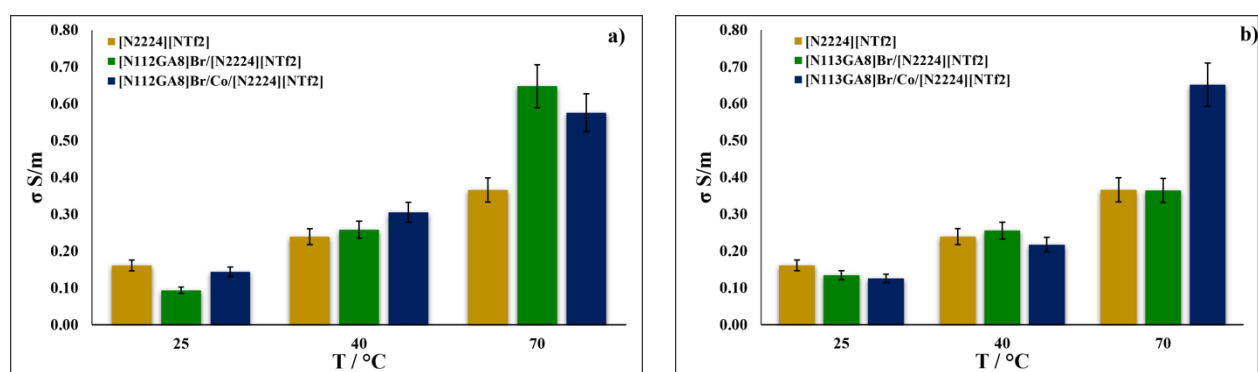

Figure 9. Conductivity (σ) values as a function of the temperature for thermochromic solutions and their components. **a)** $[N_{1\,1\,2GA\,8}]Br/Co(NTf_2)_2/[N_{2\,2\,2\,4}][NTf_2]$ (3:1). The film contains 85% of PMMA ; b) $[N_{1\,1\,3GA\,8}]Br/Co(NTf_2)_2/[N_{2\,2\,2\,4}][NTf_2]$ (3:1). The film contains 84% of PMMA.

Interestingly, thermochromic systems retain conductive behaviour typical of an IL solvent and, both at 25 and 40 °C, σ values for thermochromic solutions were comparable to that of an IL solvent. At 70 °C a different situation was recorded, as the system showed σ values significantly higher than the ones detected for the IL solvent or ligand solution.

However, in the presence of $[N_{1\,1\,2GA\,8}]$Br, the above increase seems to be due to an increase in σ value corresponding to the ligand. Conversely, for $[N_{1\,1\,3GA\,8}]$Br , it can be reasonably argued that this is a peculiar feature of the thermochromic system.

Data relevant to the thermochromic films prepared with 85 and 84 % of PMMA are reported in Figure 10, together with σ values corresponding to PMMA.
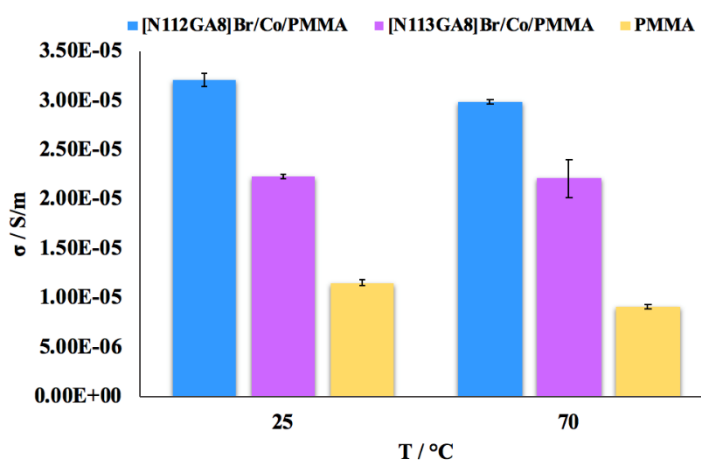
Figure 10. Conductivity (σ) values at variable temperature for PMMA layer and thermochromic films: $[N_{1\,1\,2GA\,8}]$Br/Co(NTf$_2$)$_2$/PMMA (3:1) (85% of PMMA), $[N_{1\,1\,3GA\,8}]$Br/Co(NTf$_2$)$_2$/PMMA (3:1) (84% of PMMA).

In general, contrary to what was detected in the solution, the increase in temperature does not affect the conductivity values. Obviously, thermochromic systems exhibit higher conductivity values than PMMA polymer, but in this case a significant contribution deriving from the ligand nature was detected, as accounted for by the higher values measured for $[N_{1\,1\,2GA\,8}]$Br/Co(NTf$_2$)$_2$/PMMA (3:1) than for $[N_{1\,1\,3GA\,8}]$Br/Co(NTf$_2$)$_2$/PMMA (3:1).

Conclusions

The search for new smart materials to be applied in energy saving is a topic of current interest with the aim to decrease modern societies dependency on fossil fuels. The efficiency and environmental impact of the components are imperative in designing such kind of materials.

With the above premises in mind, we analysed the thermochromic interaction between Co(II) and some sugar-based ILs recently synthesised.[39] Our investigation demonstrated how the right modulation of the IL ligand structure can be the key point to obtain self-containing systems exhibiting thermochromic behaviour in a mild range of temperature that goes from 45

up to 59 °C, changing the ligand structure and the solvent nature. These systems exhibit a change in colour from pink to light blue, ascribable to a change in the cobalt coordination sphere from octahedral to tetrahedral, as accounted for by the VT NMR and the magnetic susceptibility investigation.

Interestingly, the thermochromic behaviour was also retained when the cobalt complex was embedded in a PMMA polymeric matrix, obtaining thin films. These latter retained their conductive properties, which is generally a feature of IL-based systems, but contrary to the corresponding solutions, conductivity values were not affected by temperature. The performance of the films improved in parallel to the increased polymer count. An investigation performed on the recycling of the thin films demonstrated that the $[N_{1\,1\,3GA\,8}]Br/Co(NTf_2)_2$ (3:1)/PMMA film can be reused for 42 cycles over three months, without any loss in performance and also after 420 days of storage in air. The performance of these systems has led us to believe that besides the application of the technology in smart windows, they could be also used as coatings in automotive glass or eyeglasses.

The aim of understanding more about the modulation of the thermochromic behaviour of cobalt systems with ILs as ligands has been achieved. All of these results could be beneficial to the design of new ligands for smart materials in future applications, opening the possibility of obtaining self-contained thermochromic systems with the aim of reducing the use of carbon sources and environmental preservation. With this in mind and if the IL ligands proved to be eco- and biocompatible,[39] the overall environmental impact of the systems depends also on the nature of the IL used as the solvent, the metal salt used and the performance as measured in a real apparatus. These are clearly aspects to be investigated and improved in the future, to maximize the advantages coming from the systems resilience.

On this subject, the ligand structure, rich in hydrogen bonds and van der Waals interaction sites, could offer an opportunity to entrap the thermochromic complex in a soft material matrix, like a gel phase which could reduce or avoid the leaching issues that sometimes occurs in these types of systems. This could be used as the basis for further study in this area.

Experimental Section

Materials

Poly(methyl methachrylate), $[N_{2\,2\,2\,4}][NTf_2]$ (99.0%), $[C_1C_4pyrr][NTf_2]$ (≥98.5%), $[N_{1\,1\,1\,3}][NTf_2]$ (>98.0%), $Co(NTf_2)_2$, Potassium chloride, 0.117M (Conductivity Standard) were purchased and used without further purification. $[N_{112GA8}]Br$, $[N_{112GA8L}]Br$, $[N_{113GA8}]Br$,

[N$_{112GA12}$]Br and [N$_{112GA4}$]I were synthesised according to a previous reported procedure.[39] Ionic liquids and ligands were dried under high vacuum at 60 °C, before the use. Dichloromethane (> 99.8 %) was purchased and used without further purification.

Preparation of the thermochromic solution

Co(NTf$_2$)$_2$ salt (5.75 mg, 9.28·10^{-3} mmol) was dissolved in an IL (600 mg). In order to assist solubilisation, the suspension was sonicated with an ultrasound bath (VWR ultrasonic cleaning bath and Decon ultrasonics Ltd.), working at 45 kHz, for 30 min. A pink homogeneous solution was obtained, to which the proper IL-ligand at the desired molar ratio was added. The mixture was heated at 90 °C for 1.5 h.

Preparation of the thermochromic film

The proper ligand (0.11 mmol) and Co(NTf$_2$)$_2$ (23 mg, 0.037 mmol) were solubilised in DCM (3 mL). The polymer (390/340/290 mg) was solubilised in DCM (8 mL). In order to obtain homogeneous solutions, the mixtures were sonicated for 30 min. After cooling to room temperature, they were mixed, obtaining a pink solution. This solution was placed in a Petri dish (diameter: 10 cm). The solvent slowly evaporated at room temperature. A pink homogeneous film was obtained that was subsequently removed from the glass by peeling. The films contained mass fraction of PMMA ranging from 85 down to 81% for [N$_{112GA8}$]Br/Co(NTf$_2$)$_2$ and from 84 down to 81% for [N$_{113GA8}$]Br/Co(NTf$_2$)$_2$.

UV-vis measurements

UV-vis spectra of the solutions were recorded with a Beckman Coulter DU 800 spectrophotometer, equipped with a Peltier temperature controller. The solution was placed in a quartz cuvette with light path of 0.2 cm. Spectra were recorded in the wavelength range 250-900 nm. Spectra of the film were recorded using the Agilent Cary 60 UV-Vis spectrophotometer equipped with a temperature control block, where a quartz cuvette, having a light path of 0.2 cm and containing the film, was placed. Spectra were recorded in the wavelength range 300-800 nm.

Preparation of the sample for the Evans method[49]

The thermochromic solution was prepared according to the procedure described above. *t*-butanol or DMF (0.2 mL) was added to the solution and the obtained mixture was transferred into an NMR tube. Additionally, two coaxially capillaries containing the solvent reference (*t*-

butanol/DMF and DMSO-d_6) were placed inside the NMR tube. The X_m and the μ_{eff} were calculated using the procedure reported in Supporting Information.

NMR measurements

The VT ^{59}Co NMR were recorded using the Ascend™ 600 Bruker with an internal reference solvent (K$_3$[Co(CN)$_6$] in D$_2$O in a sealed silica capillary). Spectra were recorded from 293.15 to 363.15 K, with a temperature gradient of 10 K. Before each measurement, the sample was equilibrated for 20 min.

The VT ^{1}H NMR spectra for the Evans method were recorded using two internal reference solvents (DMSO-d_6 and t-butanol/DMF). Also, in this case, before each measurement, the sample was equilibrated for 20 min. A temperature gradient of 10 K was used.

Thermogravimetric analysis

Thermogravimetric analysis was performed using TA instrument Discovery TGA. Samples were placed in a Platinum HT pan, and heated at a rate of 5 °C min^{-1} under a dinitrogen atmosphere. The onset of weight loss in each thermogram was used as a measure of the decomposition temperature (point at 5 wt% loss of the sample).

Conductivity measurements

The electrical conductivities σ (S/m) of thermochromic solutions and films were measured with a Autolab potentiostat. The electrochemical impedance spectroscopy measurements were performed applying 0.01 V potential bias to the cell, with frequencies varying from 1×10^5 Hz to 0.1 Hz. The resistance of each sample was determined through the Nyquist plot.[60] The cell constant K for the liquid cell was calculated using a standard solution of KCl. The cell constant for the film cell was calculated experimentally, using the cell size and the thickness of the polymer film.

Acknowledgements

ASSOCIATED CONTENT

Supporting Information.

Magnetic susceptibility calculations, conductivity data, VT UV-vis spectra and colour shades for thermochromic solutions, VT NMR investigations, Job's plots and VT UV-vis spectra for thermochromic films. The following files are available free of charge at https://pubs.acs.org

AUTHOR INFORMATION

Corresponding Authors

*Prof. Francesca D'Anna, Università degli Studi di Palermo, Dipartimento STEBICEF, Viale delle Scienze, Ed. 17 90128 Palermo (Italy); email: francesca.danna@unipa.it; orcid.org/0000-0001-6171-8620

Authors

Floriana Billeci, Università degli Studi di Palermo, Dipartimento STEBICEF, Viale delle Scienze, Ed. 17 90128 Palermo (Italy); email: floriana.billeci@unipa.it; orcid.org/0000-0001-7485-3012

H. Q. Nimal Gunaratne, The QUILL Research Centre, School of Chemistry and Chemical Engineering, and [c] School of Chemistry and Chemical Engineering, Queen's University of Belfast, Stranmillis Road, Belfast, Northern Ireland BT9 5AG, UK; email: N.gunaratne@qub.ac.uk; orcid.org/0000-0002-4392-8322

Peter Licence, GSK Carbon Neutral Laboratories, School of Chemistry, The University of Nottingham, Nottingham, UK; email: peter.licence@nottingham@ac.uk; orcid.org/0000-0003-2992-0153

Kenneth R. Seddon, deceased

Natalia V. Plechkova, The QUILL Research Centre, School of Chemistry and Chemical Engineering, and Wellcome-Wolfson Institute for Experimental Medicine, School of Medicine, Dentistry and Biomedical Sciences, The Queen's University Belfast, 97 Lisburn

Road, BT9 7BL Belfast, U.K; email: n.plechkova@qub.ac.uk; orcid.org/0000-0003-2254-9603

Author Contributions

The manuscript was written through contributions of all authors. All authors have given approval to the final version of the manuscript.

References

(1)   Weinstein, L. A.; Loomis, J.; Bhatia, B.; Bierman, D. M.; Wang, E. N.; Chen, G. Concentrating Solar Power. *Chem. Rev. (Washington, DC, U. S.)* **2015**, *115*, 12797-12838; 10.1021/acs.chemrev.5b00397

(2)   Zhang, H.; Baeyens, J.; Cáceres, G.; Degrève, J.; Lv, Y. Thermal energy storage: Recent developments and practical aspects. *Progr. Energy Combust. Sci.* **2016**, *53*, 1-40; https://doi.org/10.1016/j.pecs.2015.10.003

(3)   Gur, I.; Sawyer, K.; Prasher, R. Searching for a Better Thermal Battery. *Science* **2012**, *335*, 1454-1455; 10.1126/science.1218761

(4)   Kucharski, T. J.; Tian, Y.; Akbulatov, S.; Boulatov, R. Chemical solutions for the closed-cycle storage of solar energy. *Energy Environ. Sci.* **2011**, *4*, 4449-4472; 10.1039/C1EE01861B

(5)   Gurke, J.; Quick, M.; Ernsting, N. P.; Hecht, S. Acid-catalysed thermal cycloreversion of a diarylethene: a potential way for triggered release of stored light energy? *Chem. Commun.* **2017**, *53*, 2150-2153; 10.1039/C6CC10182H

(6)   Huang, J.; Jiang, Y.; Wang, J.; Li, C.; Luo, W. A high energy, reusable and daily-utilization molecular solar thermal conversion and storage material based on azobenzene/multi-walled carbon nanotubes hybrid. *Thermochim. Acta* **2017**, *657*, 163-169; https://doi.org/10.1016/j.tca.2017.10.002

(7)   Jorner, K.; Dreos, A.; Emanuelsson, R.; El Bakouri, O.; Fdez. Galván, I.; Börjesson, K.; Feixas, F.; Lindh, R.; Zietz, B.; Moth-Poulsen, K.; Ottosson, H. Unraveling factors leading to efficient norbornadiene–quadricyclane molecular solar-thermal energy storage systems. *Journal of Materials Chemistry A* **2017**, *5*, 12369-12378; 10.1039/C7TA04259K

(8)   Masutani, K.; Morikawa, M.-a.; Kimizuka, N. A liquid azobenzene derivative as a solvent-free solar thermal fuel. *Chem. Commun.* **2014**, *50*, 15803-15806; 10.1039/C4CC07713J

(9)   Saydjari, A. K.; Weis, P.; Wu, S. Spanning the Solar Spectrum: Azopolymer Solar Thermal Fuels for Simultaneous UV and Visible Light Storage. *Advanced Energy Materials* **2017**, *7*, 4; https://doi.org/10.1002/aenm.201601622

(10)   Crano, J. C.; Guglielmetti, R. J.: *Organic Photochromic and Thermochromic Compounds: Volume 2: Physicochemical Studies, Biological Applications, and Thermochromism*; Springer: United States, 2006.

(11)   Andrews, D. L.: *Energy Harvesting Materials, World Scientific Publishing Ltd*, 2005.

(12)   Day, J. H. Thermochromism of inorganic compounds. *Chem. Rev. (Washington, DC, U. S.)* **1968**, *68*, 649-657; 10.1021/cr60256a001

(13)   Yuan, T.; Xu, Y.; Zhu, C.; Jiang, Z.; Sue, H.-J.; Fang, L.; Olson, M. A. Tunable Thermochromism of Multifunctional Charge-Transfer-Based Supramolecular Materials Assembled in Water. *Chem. Mater.* **2017**, *29*, 9937-9945; 10.1021/acs.chemmater.7b03273

(14)   Kalninsh, K. K. Structure and thermochromism of spiropyrans. Triplet mechanism of the thermal cleavage/closure of the pyran ring. *J. Struct. Chem.* **1998**, *39*, 642-650; 10.1007/BF02903537

(15)   Sone, K.; Fukuda, Y.: *Thermochromic and Chromotropic Phenomena of Cobalt(II) Chloride Solutions and Related Systems. In: Inorganic Thermochromism. Inorganic Chemistry Concepts*; Springer, Berlin, Heidelberg, 1987; Vol. 10. pp. 13-42.

(16)   Kohno, Y.; Cowan, M. G.; Masuda, M.; Bhowmick, I.; Shores, M. P.; Gin, D. L.; Noble, R. D. A cobalt(ii) bis(salicylate)-based ionic liquid that shows thermoresponsive and selective water coordination. *Chem. Commun.* **2014**, *50*, 6633-6636; 10.1039/C4CC01023J

(17)   Barry, N. P. E.; Deeth, R. J.; Clarkson, G. J.; Prokes, I.; Sadler, P. J. Thermochromic organometallic complexes: experimental and theoretical studies of 16- to 18-electron interconversions of adducts of arene Ru(ii) carboranes with aromatic amine ligands. *Dalton Trans.* **2013**, *42*, 2580-2587; 10.1039/C2DT32650G

(18)   Garshasbi, S.; Santamouris, M. Using advanced thermochromic technologies in the built environment: Recent development and potential to decrease the energy consumption and fight urban overheating. *Sol. Energy Mater. Sol. Cells* **2019**, *191*, 21-32; https://doi.org/10.1016/j.solmat.2018.10.023

(19)   A. Seeboth; Ruhmann, R.; Mühling, O. Thermotropic and Thermochromic Polymer Based Materials for Adaptive Solar Control. *Materials* **2010**, *3*, 5143-5168;

(20)   Binions, R.: Thermochromic Thin Films and Nanocomposites for Smart Glazing. In *Intelligent Nanomaterials*; Tiwari, A., Mishra, A. K., Kobayashi, H., Turner, A. P., Eds., 2012; pp 251-316.

(21)   Hoffmann, S.; Lee, E. S.; Clavero, C. Examination of the technical potential of near-infrared switching thermochromic windows for commercial building applications. *Sol. Energy Mater. Sol. Cells* **2014**, *123*, 65-80; https://doi.org/10.1016/j.solmat.2013.12.017

(22)   Bamfiel, P.; Hutchings, M.: *Chromic Phenomena: Technological Applications of Colour Chemistry: Edition 3*, 2018.

(23)   Nieuwpoort, W. C.; Wesselink, G. A.; van der Wee, E. H. A. M. Thermochromic and solvochromic behaviour of cobalt (II) chloride solutions in various solvents. *Recueil des Travaux Chimiques des Pays-Bas* **1966**, *85*, 397-404; 10.1002/recl.19660850411

(24)   Lei, Z.; Chen, B.; Koo, Y. M.; MacFarlane, D. R. Introduction: Ionic Liquids. *Chem Rev* **2017**, *117*, 6633-6635; 10.1021/acs.chemrev.7b00246

(25)   Shen, C.; Sheng, T.; Zhu, Q.; Hu, S.; Wu, X. Four new cobalt(ii) coordination complexes: thermochromic switchable behavior in the process of dehydration and rehydration. *CrystEngComm* **2012**, *14*, 3189-3198; 10.1039/C2CE06478B

(26)   D'Anna, F.; Nimal Gunaratne, H. Q.; Lazzara, G.; Noto, R.; Rizzo, C.; Seddon, K. R. Solution and thermal behaviour of novel dicationic imidazolium ionic liquids. *Org. Biomol. Chem.* **2013**, *11*, 5836-5846; 10.1039/C3OB40807H

(27)   Cruz, T. F. C.; Shimizu, K.; Esperança, J. M. S. S.; André, V.; Duarte, M. T.; Rebelo, L. P. N.; Gomes, P. T.; Canongia Lopes, J. N. Ionic Liquids in Wonderland: From Electrostatics to Coordination Chemistry. *J. Phys. Chem. C* **2019**, *123*, 5804-5811; 10.1021/acs.jpcc.9b00987

(28)   Rizzo, C.; D'Anna, F.; Noto, R. Functionalised diimidazolium salts: the anion effect on the catalytic ability. *RSC Adv.* **2016**, *6*, 58477-58484; 10.1039/C6RA12037G

(29)   Rizzo, C.; Marullo, S.; Dintcheva, N. T.; Gambarotti, C.; Billeci, F.; D'Anna, F. Ionic liquid gels and antioxidant carbon nanotubes: Hybrid soft materials with improved radical scavenging activity. *J. Colloid Interface Sci.* **2019**, *556*, 628-639; https://doi.org/10.1016/j.jcis.2019.08.108

(30)   Gu, C.-D.; Tu, J.-P. Thermochromic behavior of chloro-nickel(II) in deep eutectic solvents and their application in thermochromic composite films. *RSC Adv.* **2011**, *1*, 1220-1227; 10.1039/C1RA00345C

(31)   Wei, X.; Yu, L.; Jin, X.; Wang, D.; Chen, G. Z. Solar-thermochromism of Pseudocrystalline Nanodroplets of Ionic Liquid–NiII Complexes Immobilized inside Translucent Microporous PVDF Films. *Adv. Mater.* **2009**, *21*, 776-780; 10.1002/adma.200801816

(32)   Wei, X.; Yu, L.; Wang, D.; Jin, X.; Chen, G. Z. Thermo-solvatochromism of chloro-nickel complexes in 1-hydroxyalkyl-3-methyl-imidazolium cation based ionic liquids. *Green Chem.* **2008**, *10*, 296-305; 10.1039/B715763K

(33)   Banic, N.; Vranes, M.; Abramović, B.; Canadi, J.; Gadžurić, S. Thermochromism, stability and thermodynamics of cobalt(II) complexes in newly synthesized nitrate based ionic liquid and its photostability. *Dalton Trans.* **2014**, *43*, 15515-15525; 10.1039/C4DT01836B

(34)   May, B.; Hönle, M.; Heller, B.; Greco, F.; Bhuin, R.; Steinrück, H.-P.; Maier, F. Surface-Induced Changes in the Thermochromic Transformation of an Ionic Liquid Cobalt Thiocyanate Complex. *The Journal of Physical Chemistry Letters* **2017**, *8*, 1137-1141; 10.1021/acs.jpclett.7b00142

(35)   McCourt, É.; Wojnarowska, Z.; Jacquemin, J.; Nockemann, P.; Manyar, H. G.; Hawelek, L.; Paluch, M. Temperature- and Pressure-Induced Structural Changes of Cobalt(II) in a Phosphonium-Based Ionic Liquid. *J. Phys. Chem. C* **2016**, *120*, 10156-10161; 10.1021/acs.jpcc.6b01325

(36)   Osborne, S. J.; Wellens, S.; Ward, C.; Felton, S.; Bowman, R. M.; Binnemans, K.; Swadźba-Kwaśny, M.; Gunaratne, H. Q. N.; Nockemann, P. Thermochromism and switchable paramagnetism of cobalt(ii) in thiocyanate ionic liquids. *Dalton Trans.* **2015**, *44*, 11286-11289; 10.1039/C5DT01829C

(37)   Sniekers, J.; Geysens, P.; Vander Hoogerstraete, T.; Van Meervelt, L.; Fransaer, J.; Binnemans, K. Cobalt(ii) liquid metal salts for high current density electrodeposition of cobalt. *Dalton Trans.* **2018**, *47*, 4975-4986; 10.1039/C8DT00283E

(38)   Billeci, F.; Gunaratne, H. Q. N.; D'Anna, F.; Morgan, G. G.; Seddon, K. R.; Plechkova, N. V. A magnetic self-contained thermochromic system with convenient temperature range. *Green Chem.* **2019**, *21*, 1412-1416; 10.1039/C8GC03906B

(39)   Billeci, F.; D'Anna, F.; Feroci, M.; Cancemi, P.; Feo, S.; Forlino, A.; Tonnelli, F.; Seddon, K. R.; Gunaratne, H. Q. N.; Plechkova, N. V. When Functionalization Becomes Useful: Ionic Liquids with a "Sweet" Appended Moiety Demonstrate Drastically Reduced Toxicological Effects. *ACS Sustainable Chemistry & Engineering* **2020**, *8*, 926-938; 10.1021/acssuschemeng.9b05507

(40)   Miessler, G. L.; Tarr, D. A.: *Inorganic Chemistry*; Prentice Hall: New Jersey, 1998.

(41)   Berlett, B. S.; Levine, R. L.; Stadtman, E. R. Use of Isosbestic Point Wavelength Shifts to Estimate the Fraction of a Precursor That Is Converted to a Given Product. *Anal. Biochem.* **2000**, *287*, 329-333; https://doi.org/10.1006/abio.2000.4876

(42)   Hajime, M.; Masahiro, Y.; Kazumi, T.; Masakatsu, N.; Yukiko, K.; Yoshinori, M. Highly Conductive Room Temperature Molten Salts Based on Small Trimethylalkylammonium Cations and Bis(trifluoromethylsulfonyl)imide. *Chem. Lett.* **2000**, *29*, 922-923; 10.1246/cl.2000.922

(43)   Lee, C.-P.; Peng, J.-D.; Velayutham, D.; Chang, J.; Chen, P.-W.; Suryanarayanan, V.; Ho, K.-C. Trialkylsulfonium and tetraalkylammonium cations-based ionic liquid electrolytes for quasi-solid-state dye-sensitized solar cells. *Electrochim. Acta* **2013**, *114*, 303-308; https://doi.org/10.1016/j.electacta.2013.09.087

(44)   Billeci, F.; D'Anna, F.; Gunaratne, H. Q. N.; Plechkova, N. V.; Seddon, K. R. "Sweet" ionic liquid gels: materials for sweetening of fuels. *Green Chem.* **2018**, *20*, 4260-4276; 10.1039/C8GC01615A

(45)   Marusak, R. A.; Doan, K.; Cummings, S. D.: Werner's Notion—Creating the Field: Synthesis and Analysis of Cobalt Ammine Coordination Compounds1–15. In *Integrated Approach to Coordination Chemistry*; Wiley, 2006; pp 22-51.

(46)   Sharutin, V. V.; Senchurin, V. S.; Sharutina, O. K.; Kunkurdonova, B. B. Synthesis and structure of cobalt complexes [Me3EtN]2+[CoI4]2− and [Me3BuN]2+[CoI4]2−. *Russ. J. Inorg. Chem.* **2011**, *56*, 1384-1389; 10.1134/S0036023611090245

(47)   Renny, J. S.; Tomasevich, L. L.; Tallmadge, E. H.; Collum, D. B. Method of continuous variations: applications of job plots to the study of molecular associations in organometallic chemistry. *Angewandte Chemie (International ed. in English)* **2013**, *52*, 11998-12013; 10.1002/anie.201304157

(48)   Karlin, K. D.: *Progress in Inorganic Chemistry, Volume 29*; Wiley: New York, 1982.

(49)   Evans, D. F. 400. The determination of the paramagnetic susceptibility of substances in solution by nuclear magnetic resonance. *Journal of the Chemical Society (Resumed)* **1959**, 2003-2005; 10.1039/JR9590002003

(50)   Chauvin, Y.; Gilbert, B.; Guibard, I. Catalytic dimerization of alkenes by nickel complexes in organochloroaluminate molten salts. *J. Chem. Soc., Chem. Commun.* **1990**, 1715-1716; 10.1039/C39900001715

(51)   Cotton, F. A.; Wilkinson, G.: *Advanced Inorganic Chemistry*; Third ed.: United States, 1972.

(52)   Nicholls, D.: 41 - COBALT. In *The Chemistry of Iron, Cobalt and Nickel*; Nicholls, D., Ed.; Pergamon: UK, 1973; pp 1053-1107.

(53)   McClintock, L. F.; Bagaria, P.; Kjaergaard, H. G.; Blackman, A. G. Co(III) complexes of the type [(L)Co(O2CO)]+ (L=tripodal tetraamine ligand): Synthesis, structure, DFT calculations and 59Co NMR. *Polyhedron* **2009**, *28*, 1459-1468; https://doi.org/10.1016/j.poly.2009.03.010

(54)   Medek, A.; Frydman, V.; Frydman, L. Solid and liquid phase 59Co NMR studies of cobalamins and their derivatives. *Proc. Natl. Acad. Sci. U. S. A.* **1997**, *94*, 14237-14242; 10.1073/pnas.94.26.14237

(55)   Ozvat, T. M.; Peña, M. E.; Zadrozny, J. M. Influence of ligand encapsulation on cobalt-59 chemical-shift thermometry. *Chem. Science* **2019**, *10*, 6727-6734; 10.1039/c9sc01689a

(56)   Freeman, R.; Murray, G. R.; Richards, R. E.; Thompson, H. W. Cobalt nuclear resonance spectra. *Proceedings of the Royal Society of London. Series A. Mathematical and Physical Sciences* **1957**, *242*, 455-466; doi:10.1098/rspa.1957.0188

(57)   Xu, Z.; Wang, S.; Hu, X.-Y.; Jiang, J.; Sun, X.; Wang, L. Sunlight-Induced Photo-Thermochromic Supramolecular Nanocomposite Hydrogel Film for Energy-Saving Smart Window. *Solar RRL* **2018**, *2*, 1800204; 10.1002/solr.201800204

(58)   Salamati, M.; Kamyabjou, G.; Mohamadi, M.; Taghizade, K.; Kowsari, E. Preparation of TiO2@W-VO2 thermochromic thin film for the application of energy efficient smart windows and energy modeling studies of the produced glass. *Construction and Building Materials* **2019**, *218*, 477-482; https://doi.org/10.1016/j.conbuildmat.2019.05.046

(59)   Liu, P.; Liu, L.; Jiang, K.; Fan, S. Carbon-Nanotube-Film Microheater on a Polyethylene Terephthalate Substrate and Its Application in Thermochromic Displays. *Small* **2011**, *7*, 732-736; 10.1002/smll.201001662

(60)   Bavafa-Toosi, Y.: 6 - Nyquist plot. In *Introduction to Linear Control Systems*; Bavafa-Toosi, Y., Ed.; Academic Press, 2019; pp 533-640.

TOC
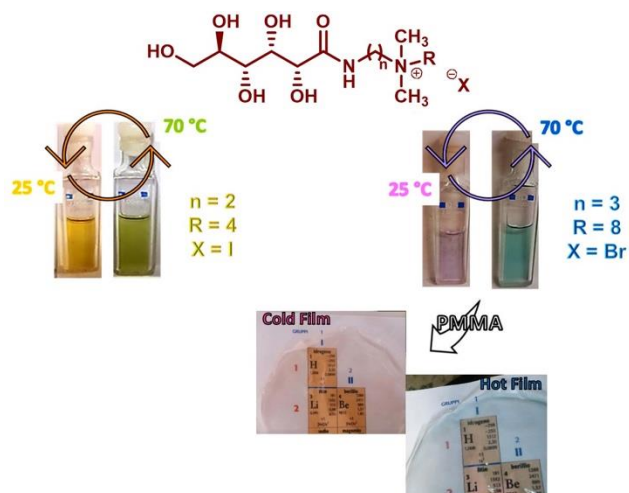
Self-contained thermochromic systems operating in accessible temperature ranges were obtained combining properties of a Co(II) salt and sugar-based ionic liquids.